

Nature of the highest energy cosmic rays

Todor Stanev

Bartol Research Institute, University of Delaware, Newark, Delaware 19716

H. P. Vankov

Institute for Nuclear Research and Nuclear Energy, Sofia 1184, Bulgaria

(Received 24 June 1996)

Ultrahigh energy γ rays produce electron-positron pairs in interactions on the geomagnetic field. The pair electrons suffer magnetic bremsstrahlung and the energy of the primary γ ray is shared by a bunch of lower energy secondaries. These processes reflect the structure of the geomagnetic field and cause experimentally observable effects. The study of these effects with future giant air shower arrays can identify the nature of the highest energy cosmic rays as either γ rays or nuclei. [S0556-2821(97)05003-0]

PACS number(s): 98.70.Sa, 91.25.Cw, 96.40.De, 96.40.Pq

I. INTRODUCTION

Ever since the reports of the detection of two cosmic ray showers of energy well above 10^{20} eV [1,2] the origin and the nature of such events have been the subject of strong interest and intense discussion. It is not only very difficult [3] to extend our understanding of particle acceleration to such extraordinarily high energies but the propagation of these particles in the microwave background and possibly other universal radiation fields restricts the distance to their potential sources to several tens of Mpc.

Conservatively minded astrophysicists are looking for astrophysical sources which may contain the environment necessary for stochastic particle acceleration to energies in excess of 10^{20} eV. Powerful Fanaroff-Riley class II (FR II) radio galaxies [4] have been suggested as possible sources. If this suggestion were true, the highest energy cosmic rays (HECR's) would be the most likely protons, reflecting the composition of the matter that is available for injection in the termination shocks of FR II jets. Others [5] search for powerful astrophysical sources in the cosmologically nearby universe. HECR then could also be heavier nuclei, for which the acceleration is less demanding. The propagation of heavy nuclei on short distances (~ 10 Mpc) without huge energy loss is possible.

Some cosmologists relate the origin of HECR's to topological defect [6]. Topological defects (TD) scenarios avoid the problems of particle acceleration since they are based on "top-down" evolution. Very massive (10^{22} – 10^{25} eV) X particles are emitted by the topological defects that later decay into baryons and mesons of lower energy. Most of the energy is eventually carried by γ rays and neutrinos that are products of meson decay. Detected HECR's would then most likely be γ rays.

Most radically, the origin of the HECR has been related to those of gamma-ray bursts [7–9], replacing two extremely luminous mysteries with a single one. In such scenarios HECR's are most likely to be protons again. We may not be able to observe the sources of the HECR since every source might only emit a single observed ultrahigh energy particle.

The nature, the type of the particle that interacted in the atmosphere to generate these giant air showers could be the

key to understanding the origin of the highest energy cosmic rays. The current experimental evidence on the nature of the HECR is not conclusive. The Fly's Eye experiment, for example, has reported correlated changes in the spectra and the composition of the ultrahigh energy cosmic rays [10]. The analysis of the Fly's Eye experimental statistics suggests that a change of the chemical composition of the cosmic rays from heavy nuclei to protons at $\sim 3 \times 10^{18}$ eV is accompanied by a change of the spectral index of the cosmic ray energy spectrum. One may then conclude that the HECR's are protons. The other currently running air shower experiment, the Akemo Giant Air Shower Array (AGASA), does not observe [11] such a correlation. A reanalysis of the archival data from the Sydney University Giant Air Shower Recorder (SUGAR) experiment [12] makes the opposite conclusion, a large fraction of the highest energy showers seem to be generated by heavy nuclei.

A correlation between the arrival directions of the HECR with energy $> 4 \times 10^{19}$ eV with the supergalactic plane, that is the plane around which most of the galaxies of redshift < 0.03 are concentrated, has been reported [13]. The AGASA experiment [14] has also observed a strong anisotropy and correlations with the supergalactic plane, although not fully consistent with the conclusions of [13]. On the other hand, the Fly's Eye experiment does not see such a correlation [Sommers for the Fly's Eye group (private communication)]. It also has not been observed in the SUGAR data [15]. Even if confirmed in the future, a correlation with the structure of the local universe would not answer the question of the nature of HECR's. If topological defects are seeds for galaxy formation, the most powerful galaxies and TD's would have similar distribution and TD's and astrophysical scenarios of the origin of HECR's are indistinguishable.

The profile of the 3×10^{20} eV shower detected by the Fly's Eye develops higher in the atmosphere than expected for either proton or γ -ray showers of that energy [16]. The highest energy shower seen by the AGASA experiment (2×10^{20} eV) exhibits, apart from its energy, features that are typical for most of the high energy showers. The currently existing air shower arrays cannot drastically increase the experimental statistics and the hope for answering the important questions for the nature and origin of the HECR is in the

construction of much bigger shower arrays, such as the Auger project [17].

Even with Auger, however, the nature of HECR will be difficult to study. Shower parameters are the subject of strong intrinsic fluctuations and the cross sections that govern inelastic interactions at $\sqrt{s} = 100$ TeV are not known well enough. At lower energy ($10^{14} - 10^{16}$ eV) showers generated by heavy nuclei, protons, and γ rays could be at least statistically distinguished by their muon content. γ -ray showers have, on the average, $\sim 3\%$ of the muon content of proton showers of the same energy [18]. At ultrahigh energies, such an approach may not be possible—calculations of the muon content of the γ -ray induced showers predict that the fraction of GeV muons could be even higher than in proton generated showers [19,20].

We suggest a different approach to the study of the nature of the cosmic rays with energy above 10^{19} eV—to prove (or disprove) that HECR are γ rays by observing their interactions with the geomagnetic field. While protons and heavier nuclei are not affected by the geomagnetic field, ultrahigh energy γ rays interact on it to produce e^+e^- pairs. The electrons themselves quickly lose their energy through magnetic bremsstrahlung (synchrotron radiation) before they enter the atmosphere of the earth. Air showers are thus replaced by “magnetic + atmospheric” showers that start far away from the surface of the earth and are absorbed faster compared to usual air showers. With high experimental statistics one can observe the interactions of ultra high energy γ rays with the geomagnetic field by a study of the shower arrival direction in geographical coordinates. If the detected showers do not show signs of interactions with the geomagnetic field, the suggestions for the γ -ray nature of the HECR could be proven wrong.

This work is organized in the following way. Section II gives a brief discussion of the photon and electron interactions on magnetic fields and of the structure of the geomagnetic field. Section III describes a calculation of the “geomagnetic + atmospheric” cascades and gives some general results of that calculation. Section IV calculates shower parameters that could be used to confirm the γ -ray origin of the HECR and Sec. V contains the conclusions from this research.

II. PHOTON AND ELECTRON INTERACTIONS IN THE GEOMAGNETIC FIELD

Interactions of photons, and especially of electrons, on magnetic fields have been exhaustively studied because of all the problems they create in particle accelerators. The theoretical and some experimental knowledge is reviewed by Erber in [21].

Magnetic pair production is guided by the parameter $Y_\gamma \equiv [1/2][h\nu/mc^2][B_\perp/B_{cr}]$, where $B_{cr} \equiv m^2c^3/e\hbar = 4.414 \times 10^{13}$ G and B_\perp is the component of the magnetic field that is normal to the γ -ray trajectory. The γ -ray attenuation coefficient, i.e., the fraction of photons that undergo pair production in magnetic field of strength B_\perp per unit distance, is given by

$$\alpha_\gamma(Y_\gamma) = 0.16 \frac{amc}{\hbar} \frac{mc^2}{h\nu} K_{1/3}^2(2Y_\gamma/3). \quad (1)$$

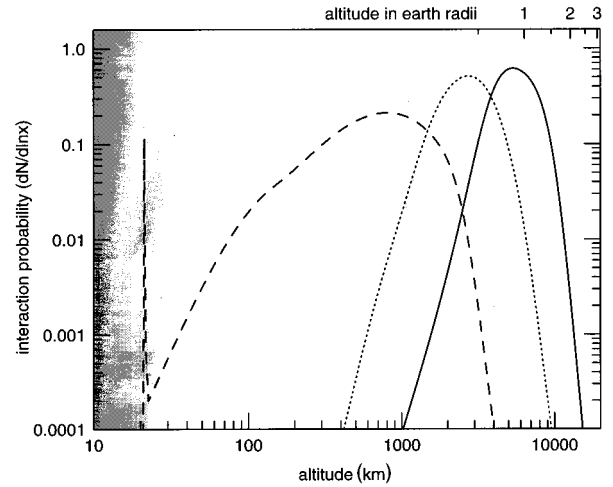


FIG. 1. Distribution of the interaction points of γ rays of energy 10^{21} eV (solid line), 3.16×10^{20} eV (dotted line), and 10^{20} eV (dashed line). The interaction points are the vertical distances from the surface of the Earth. The shading on the left-hand side of the figure represents the atmosphere.

The maximum attenuation is reached at a γ -ray energy of $12mc^2(B_{cr}/B_\perp)$ while the cross section of the process is linearly proportional to the magnetic field strength B_\perp .

Similarly the magnetic bremsstrahlung (synchrotron radiation) is guided by $Y_e \equiv [E/mc^2][B_\perp/B_{cr}]$. The radiation emitted by an electron of energy E_e in the magnetic field B_\perp per unit distance is distributed as

$$I(E_e, h\nu, B_\perp) = \frac{\sqrt{3}\alpha}{2\pi} \frac{m^2c^3}{\hbar} \frac{Y_e}{E} \left(1 - \frac{h\nu}{E_e}\right) \kappa(2J), \quad (2)$$

where $J \equiv [h\nu/E_e][1 + h\nu/E_e]/3Y_e$ and κ is incomplete Bessel function integral [21].

To demonstrate the strength of the γ -ray interactions in the geomagnetic field we show in Fig. 1 the distributions of the distances from the surface of the earth at which γ rays of different energy pair produce. The γ -ray trajectory is taken to be normal to the field lines of a magnetic dipole centered at the center of the Earth with a magnetic moment of 8.1×10^{19} Gm. One could see that the γ rays of the energies of interest interact in a relatively narrow range of distances not further than $3R_\oplus$. The narrow peak plotted at altitude of 20 km represents γ rays that survive, i.e., interact in the atmosphere before they interact in the geomagnetic field. 12% of the γ rays with energy 10^{20} eV (and none at higher energy) survive.

The spectra of the γ rays emitted in magnetic bremsstrahlung depends quite strongly on the magnetic field strength. For strong fields the energy distribution of the secondary photons is quite flat. Figure 2 shows the energy loss of 10^{20} electrons in magnetic fields of strength $\log_{10} B_\perp = -0.5, -1, -1.5$, etc., G as a function of the secondary photon energy. In the dipole field model described above a field of 0.1 G corresponds to a distance of $0.468R_\oplus$ above the surface of the Earth, and 0.032 G to $1.15R_\oplus$. These distances cover much of the primary γ -ray interaction range shown in Fig. 1. Since a lower energy

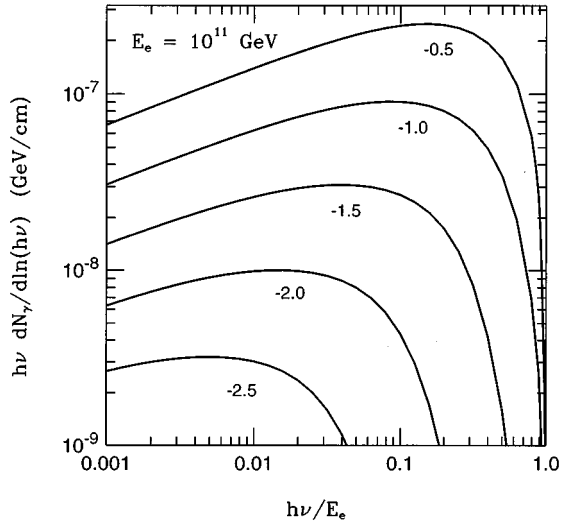


FIG. 2. Energy loss of 10^{20} eV electrons as a function of the strength of the magnetic field and the energy of the secondary photons. The field strength is indicated by the respective curve as $\log_{10}(B_{\perp}/G)$.

γ -ray pair produces close to the Earth, the magnetic bremsstrahlung of their secondary electrons is harder.

γ rays arriving at any experimental location under a different zenith (ϑ) and azimuthal (ϕ) angle will see a different geomagnetic field. They will thus cascade differently before reaching the atmosphere. At small ϑ , close to the vertical direction, the variation with ϕ is insignificant. At relatively large ϑ , more than 30° , the field strength for most locations changes by factors of 3 or more for different values of ϕ .

A more quantitative calculation of the strength of the field encountered by the incoming γ ray is trivial for any model of the geomagnetic field but has to be performed for each location ϑ and ϕ separately. We have attempted to obtain a slightly more general measure for several experimental locations. Figure 3 shows the transverse component (B_{\perp}) of the geomagnetic field as a function of the azimuthal angle at which it arrives to the detector. Since the ϕ variations for different zenith angles ϑ have the same aspect, we have integrated over ϑ from 0° to 60° , weighting the field values with the solid angle. The 1991 International Geomagnetic Reference Field model (IGRF) [22] is used for this calculation.

Four of the locations for which B_{\perp} is shown are in the northern hemisphere and only one (Sydney, shown with a dash-dashed line) is south of the equator. Since the smallest B_{\perp} is seen in the direction of the magnetic pole that is closer to each location, northern and southern locations have opposite field strength dependence on ϕ . At the moderate latitudes of these detector locations, the detailed differences between the northern hemisphere detectors are minor. (A detector located at the geomagnetic equator would have a symmetric response to geomagnetic north and south directions.) The difference between the maximum and minimum field strengths is almost a factor of 5.

For each one of these detectors, as well as for any other detector location, one could determine a region in azimuth,

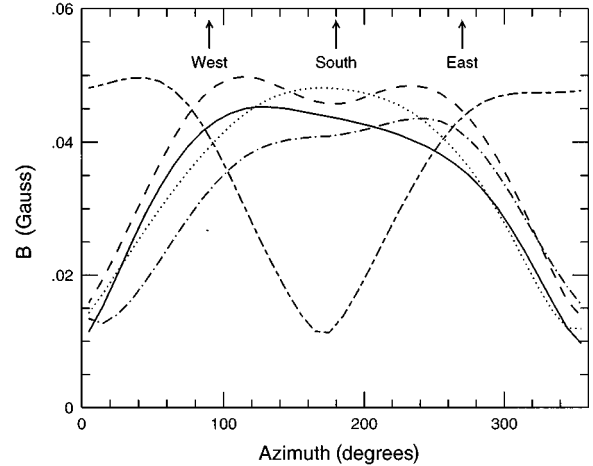


FIG. 3. The strength of the geomagnetic field component that is perpendicular to the γ -ray trajectory as a function of the azimuthal angle ϕ at which the particle arrives at the location is shown for a distance of $1R_{\oplus}$ from the detector. The field strength is integrated over zenith angles ϑ from 0° to 60° accounting for the solid angle. The calculation is performed for the locations of several air shower arrays: (a) Fly's Eye (40N, 112W), solid line; (b) Yakutsk (62N, 129E), dots; (c) Akeno (35N, 138E), dashes; (d) Haverah Park (54N, 2W), dash-dotted; (e) Sydney (30S, 150E), dash-dashed. The 1991 IGRF model of the geomagnetic field is used in this calculation.

where the field strength is the lowest and the incoming γ rays would be affected minimally by the geomagnetic field and a region where the effect of the geomagnetic field is at maximum. For the location of Sydney, e.g., γ rays arriving with $130^\circ < \phi < 215^\circ$ would see $B_{\perp} < 0.02$ G at a distance of $1R_{\oplus}$ and γ rays with $255^\circ < \phi < 90^\circ$ would see more than 0.04 G at the same distance. The idea is that γ -ray fluxes arriving from these two regions may have observable characteristics that are different enough to be distinguished experimentally. We continue to study the cascading of ultra-high energy γ rays in geomagnetic fields with different strength, corresponding to these two regions.

III. CASCADING IN THE GEOMAGNETIC FIELD

We simulate the electromagnetic cascading in the geomagnetic field by injecting γ rays of energy E_{γ}^0 at a distance of $5R_{\oplus}$ from the surface of the earth on a trajectory with angle ϑ relative to the vertical direction at the intersection with the surface. The γ ray is propagated with a stepsize Δx (from 1 to 10 km) until the γ -ray pair produces or reaches the atmosphere. The atmosphere is defined to be at altitude of 20 km above the Earth's surface. Gamma rays that reach the atmosphere "survive" and interact in the atmosphere to produce air showers with their original injection energy.

If the γ ray produces an electron-positron pair, the pair electrons are followed in a similar way, by calculating their radiation spectrum on every step of propagation. The synchrotron γ rays are tabulated in energy, starting at 10^{14} eV. The assumption here is that secondary γ rays of energy less than 10^{14} eV do not contribute significantly to the cascades that are observed deep in the atmosphere. This lower energy

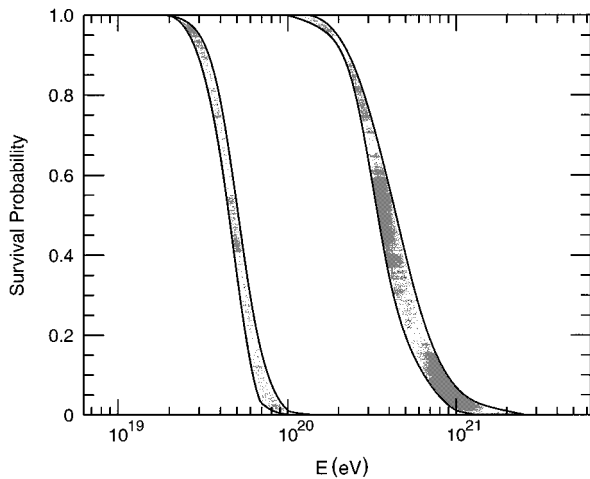


FIG. 4. Survival probability for γ rays of energy between 10^{19} and 10^{21} eV in the dipole geomagnetic field model described in the text with scaling factors of 0.25 (right-hand strip) and 1.25 (left-hand strip). The left-hand edge of each strip shows the survival probability for γ rays approaching the surface of the Earth with a zenith angle $\vartheta = 60^\circ$ and the right-hand edges are for $\vartheta = 0^\circ$.

end of the magnetic bremsstrahlung spectrum, as well as the electrons of energy below 10^{14} eV that enter the atmosphere, always contain less than 2% of the primary γ -ray energy.

Each particle produced in the geomagnetic field, as well as the “surviving” primary γ rays then generate atmospheric cascades. The profiles of these cascades are added up to calculate the composite shower profile, generated in the atmosphere by the injected primary γ ray or the products of its interaction in the geomagnetic field.

The actual calculation is performed using the dipole magnetic field model with a magnetic moment of 8.1×10^{19} G/m with two scale factors of 0.25 (low field) and 1.25 (high field). At a distance of $1R_\oplus$ above the surface of the Earth, the field strengths are 9.8×10^{-3} and 4.9×10^{-2} G, respectively, approximately equal to the maximum and minimum values shown in Fig. 3. To study the “survival” probability in these two field models, we made calculations for two extreme trajectories: $\vartheta = 0^\circ$ (particle trajectory normal to the

magnetic field line) and 60° (particle trajectory is in the plane of the field line at an angle of 60° to it). Since the exact locations and properties of the future air shower arrays are not yet known, these calculations are intended to demonstrate the plausibility of the suggested technique. Figure 4 shows the survival probabilities at high (left-hand strip) and low magnetic field strengths. The left-hand boundary of each strip corresponds to propagation at $\vartheta = 60^\circ$ and the right-hand boundary is for $\vartheta = 0^\circ$. γ rays approaching the Earth at higher zenith angles spend significantly more time in higher geomagnetic field strengths and have a higher interaction probability. The left-hand edge of the high field strip and the right-hand edge of the low field strip practically bracket the survival probability space for γ rays approaching any location at the Earth’s surface with zenith angles smaller than 60° . γ rays arriving at higher angles may be absorbed faster.

Several calculations of the γ ray cascading in the geomagnetic field have been previously performed [23,20,24]. Our results are in a good agreement with the main results of all of them. Our calculation is generally a refinement of previous ones, which nevertheless reveals some practically important features in the cascading process. Previous calculations conclude that there will be a “cutoff” in the energy spectrum of the γ rays that reach the atmosphere, because of the very soft spectrum of the secondary photons, generated by magnetic bremsstrahlung. This conclusion is partially due to the relatively rough treatment and low statistics in the previous work. Figure 5 shows the number of secondary γ rays and the energy that they carry. $E_\gamma^0 = 3 \times 10^{20}$ eV in this example. Although the number of secondary γ rays of energy above 10^{19} eV is on the average only 6.3, they carry 48% of the primary energy. This is also important for the development of the subsequent air showers, because at energies above 10^{19} eV the Landau-Pomeranchuk-Migdal (LPM) effect [25], which suppresses the electromagnetic cross sections at high energy and slows the development of the air showers, becomes important in air.

IV. ATMOSPHERIC SHOWERS

γ rays of energy above 10^{19} eV, if they do exist, would only be detectable by giant air shower arrays located on the

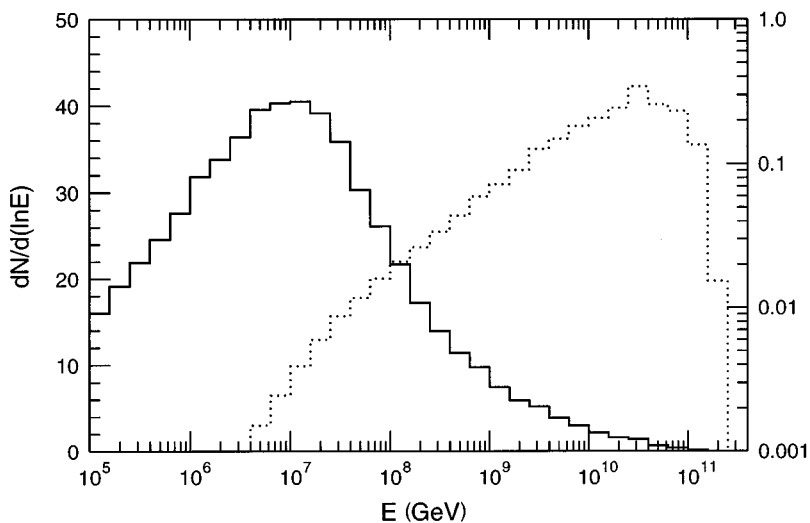


FIG. 5. Energy spectrum of the secondary γ rays that reach the atmosphere after the cascading of a primary γ ray of energy 3×10^{20} eV, solid line, left-hand scale. The dotted histogram and the right-hand scale show the amount of energy carried by the secondary γ rays in each bin.

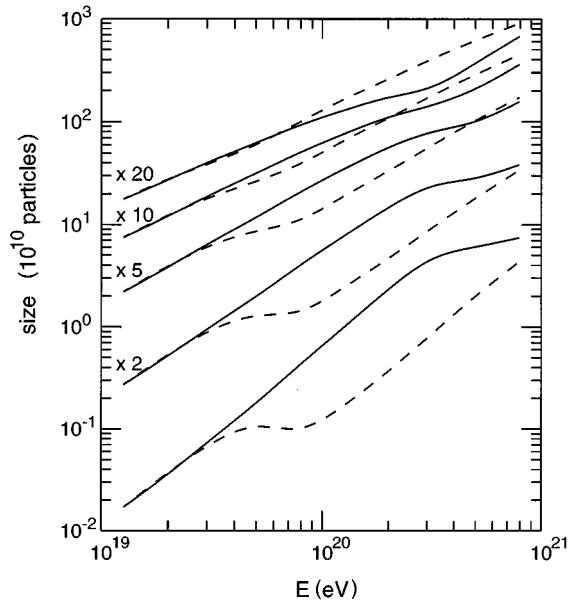


FIG. 6. Relation between the average shower size N_e and the primary γ -ray energy E_γ^0 for the five observation levels defined in the text for cascading in high (solid) and low (dashed line) strengths of the geomagnetic field. N_e values are multiplied by the factor indicated by the curves.

surface of the Earth. Air shower arrays consist of a large number of counters that trigger in coincidence when the shower front arrives. The shower direction is determined by the arrival time of the shower front at the different counters. A fit of the density in the separate counters reconstructs the total number of shower particles, the showers size N_e , which is then used to determine the primary energy.

The output of our Monte Carlo simulation includes the shower sizes calculated for several atmospheric depths from the cascading of all secondary (and primary, if the injected γ rays did not pair produce) γ rays in the atmosphere. The profiles from individual secondary γ rays of energy above 10^{18} eV are calculated with an account for the LPM effect, although the effect is not significant below 10^{19} eV. The depths are arbitrarily chosen to include a realistic range for a typical large air shower experiment and correspond to an array at a vertical depth of 860 g/cm^2 and zenith angles with $\cos\vartheta = 0.9, 0.8, 0.7, 0.6,$ and 0.5 . To a certain extent (apart from the muon content of the air showers and LPM density effects), the examples given below could also be scaled to different altitudes and zenith angles.

Figure 6 shows a general and important shower parameter—the average size ($\langle N_e \rangle$) generated by γ rays of different energy. The solid lines are for the low field (scale factor of 0.25) and the dashed lines are for the high field (scale factor of 1.25). From top to bottom the lines show $N_e(E_\gamma^0)$ at five different depths of 956, 1075, 1229, 1433, and 1720 g/cm^2 . Except for the deepest observation level, N_e is multiplied by the factor shown by each curve to make the figure readable. In the absence of interactions in the geomagnetic field, and for lower E_γ^0 the shower size has a power law dependence on E_γ , $N_e = E_\gamma^\alpha$ with $\alpha > 1$. The power law index α depends on the column density between the depth of the shower maximum X_{max} and the detector. The size at

maximum N_{max} is exactly proportional to E_γ^0 and α is bigger than unity because the depth of shower maximum grows with energy as $X_{\text{max}} = \ln(E_\gamma^0/81 \text{ MeV})$ radiation lengths (1 r.l. = 37.1 g/cm^2 in air).

The dependence shown in Fig. 6 is more complicated because in this energy range showers are already at or before their maximum development at some of the shallower observation levels. The role of the magnetic field strength on the N_e dependence on E_γ^0 is easier to understand for the deepest levels of observation. Compare, for example, the two curves for depth of 1720 g/cm^2 with the γ -ray survival probability of Fig. 4. At low energy, where there are no interactions on the geomagnetic field, the two curves are the same. The solid curve (low field) starts bending at γ -ray energy 2×10^{20} eV where the primary γ rays start interacting in the geomagnetic field. Because of these interactions the primary γ ray is replaced by a bunch of γ rays of lower energy. The composite shower reaches maximum at shallower atmospheric depths and is significantly absorbed at the deep observation level. The same happens at an energy lower by about 1 order of magnitude in the high field case. Although it is outside of the energy range of Fig. 6, at some higher energy, where all γ rays interact on the geomagnetic field, the two curves will join again.

To explain the behavior at the shallow observation levels, one has to take into account some of the details of the cascading in the geomagnetic field, namely the shape of the energy spectra of the secondary photons as a function of field strength, which is shown in Fig. 2. Although the primary γ rays interact in the same way, in the high field case the energy spectra of the secondary γ rays are harder, hard enough to generate showers that are not absorbed at the level of 956 g/cm^2 . One could hardly see a tiny deviation of the strong field (dashed) curve in the region of $E_\gamma^0 = 3 \times 10^{19}$ eV. At higher energies the secondaries are energetic enough to produce N_e dependence very close to a power law. When the primary γ rays start interacting in the low field, however, the picture is slightly different. The secondary γ -ray spectra are softer, the composite showers reach maxima at shallower depths and are correspondingly absorbed when they reach the observation level. The two curves will join asymptotically.

All other levels show intermediate behavior where the relation between the depth of observation and X_{max} also contributes to the exact shape of the curve.

Figure 6 shows the strong differences in the observable parameter N_e which is introduced by the strength of the geomagnetic field. It cannot be used, however, for analysis of experimental data because E_γ^0 is not a directly measurable parameter. What experiments can do, and usually do, is to produce a spectrum of the measured shower sizes N_e . Such spectra for the three deeper observation levels are shown in Fig. 7. The solid histogram corresponds to the low field and the dashed one to the high field case.

The histograms are result of a simulation, where E_γ^0 is sampled from a $(E_\gamma^0)^{-2}$ differential primary spectrum between 10^{19} and 10^{21} eV. At low N_e the spectra are always higher for the low field case, including the two observation levels that are not shown in Fig. 7. At the high N_e side and for shallow observation levels, the high field case shows a

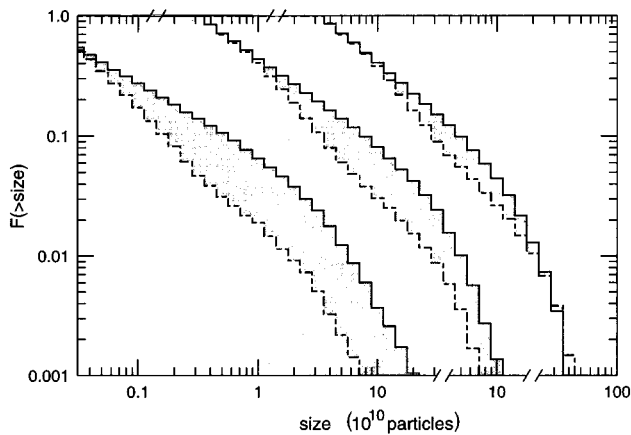


FIG. 7. Integral shower size N_e spectra generated by primary γ rays sampled on a $(E_\gamma^0)^{-2}$ differential spectrum between 10^{19} and 10^{21} eV. The solid histograms show the low field case and the dashed histograms are for the high field. The observation levels are 1720, 1433, and 1229 g/cm^2 from left to right.

higher spectrum, as could be expected by the results shown in Fig. 6 and as seen for the shallowest level plotted in Fig. 7. The biggest difference is at the deepest observation level, where the spectra are different by as much as a factor of 10. The differences between the size spectra decreases for shallower observation levels, and is probably not detectable for the two shallowest levels, which are not shown.

V. DISCUSSION AND CONCLUSIONS

The calculations presented above show the transition in the behavior of air showers initiated by primary γ rays when these γ rays start interacting on the geomagnetic field. In this sense a summary of the physics of the suggested technique is presented in Fig. 4. For the “high” field this transition starts at an energy of 2×10^{19} eV and is complete by 10^{20} eV, while for the “low” field this energy range is shifted by a factor of 5–10. For intermediate field values the shifts would be correspondingly smaller with the onset of the effect at $\sim 2 \times 10^{19}(B_{\text{high}}/B)$ eV.

The size spectra of Fig. 7 show that it is possible to detect the difference between a flux of γ rays that reach the Earth after cascading in a geomagnetic field of different effective strengths. In practical terms this means that any experiment that is able to collect large enough experimental statistics should see different N_e spectra in different azimuthal directions if HECR’s are indeed γ rays. We have not attempted to look for this effect in the existing experimental statistics, because it is not large enough to reveal such effects.

The Auger project [17] is an entirely different story. It proposes the construction of two air shower arrays, at least 3000 km^2 each, in the northern and southern hemispheres. For comparison, the area of the largest current detector (AGASA) is 100 km^2 . An inspection of Fig. 4 shows that for locations at moderate latitudes more than a half of this statistics would come from directions with $B_\perp > 0.04 \text{ G}$, i.e., with the interactions on the geomagnetic field starting at 2.5×10^{19} eV. Each one of the Auger detectors will have the collecting power of approximately 1000 showers above 2.5×10^{19} eV per year and would be able to observe the

“high field” behavior of the shower size spectra if the HECR primaries were indeed γ rays. Because of the diminishing statistics the “low field” behavior would be a non-observation of the transition.

For the northern and southern hemisphere detectors, the effects would be the strongest in opposite directions. If the southern Auger detector observes a pronounced change in the energy spectrum of showers of energy above 2.5×10^{19} eV coming from the north, the northern detectors should have the same effect in showers coming from the south.

Detectors that study the longitudinal development of air showers (Fly Eye’s type detectors) can also observe the interactions of high energy γ rays with the geomagnetic field. At energies above 10^{19} eV, γ -ray initiated air showers will develop deeper in the atmosphere because of the influence of the LPM effect. The average depth of maximum X_{max} of γ -ray showers is $1000 \text{ g}/\text{cm}^2$ at 10^{19} eV vs $950 \text{ g}/\text{cm}^2$ in the Bethe-Heitler case. At still higher energy, X_{max} of the showers coming from directions with high geomagnetic field strength would become shallower by about $200 \text{ g}/\text{cm}^2$ with the onset of the interactions on the geomagnetic field. Air showers of the same energy will also exhibit a bimodal X_{max} distribution for showers that have and have not interacted on the geomagnetic field. Showers arriving from the direction of “low field” strength would continue showing an elongation rate higher than $85.4 \text{ g}/\text{cm}^2$ typical for electromagnetic showers in the absence of the LPM effect.

The current calculation is performed to demonstrate the possibility of experimental detection of the interactions of ultrahigh energy γ rays with the geomagnetic field. For the purposes of illustration we use the highest and lowest magnetic field values calculated with a realistic field model and presented in Fig. 3. For any given array location one should define directions with distinctly different geomagnetic field values that contain most of the experimental statistics.

The actual effects may be even stronger because our simplified treatment neglects several second-order effects that may strengthen the effects of the interactions on the geomagnetic field. In the discussion of shower size spectra, we use a γ -ray propagation perpendicular to the magnetic field lines. In fact, as shown in Fig. 4, the interaction probability in the geomagnetic field increases by a non-negligible factor for some favorable particle trajectories. Our air shower simulation also does not account for the magnetic bremsstrahlung of the shower electrons which at high E_e and low atmospheric density $< 10^{-5} \text{ g}/\text{cm}^3$ could be important and could accelerate the shower development.

In principle, the interplanetary magnetic field has to be added to the “target” magnetic field. A γ ray arriving from a cone centered on the sun would be absorbed far away from the Earth and possibly not detectable. The sun could thus be visible in ultrahigh energy γ rays. The exact dimensions of the region where γ rays are absorbed in pair production on the solar magnetic field carries valuable information on the magnetic field in the vicinity of the sun. This is an interesting although purely academic problem, because the statistics of such events is always going to be negligible.

Although we have not done it for this paper, there will be effects, similar to the N_e ones, on the muon content of the γ -ray initiated air showers. It is well known that, at these extremely high energies, the number of soft muons (0.3–2

GeV) in γ initiated showers is comparable to this of hadronic showers [19,20]. The number of soft muons has an E_γ^0 dependence very similar to N_e , because the low energy muons decay readily when X_{\max} is distant from the observation level. The decay length of 1 GeV muons is ~ 6 km. A picture similar to the N_e spectra in Fig. 7 will develop as a result of the cascading in geomagnetic fields of different effective strengths. The major difference between the behavior of the electron size and the muon size is that N_e attenuates as a function of the column density, while N_μ attenuates as a function of the distance, i.e., N_μ will depend strongly on the shower zenith angle ϑ .

In short we have attempted to demonstrate that the study of the major components of the giant air showers can reveal the nature of the highest energy cosmic rays. If the specific dependence on the shower arrival direction is observed, then the highest energy cosmic rays are γ rays. A nonobservation of this effect would leave us with the choice between protons and heavy nuclei. The analysis of the experimental statistics

would, however, require Monte Carlo studies that are tuned to the exact location and capabilities of the specific air shower arrays. The geomagnetic field strength should be evaluated as a function of the zenith and azimuth angles and the shower array energy calibration and its systematic errors should be taken into account.

ACKNOWLEDGMENTS

T.S. is grateful to A. A. Watson for inspiring discussions on the subject of giant air shower. The work of T.S. was supported in part by the U.S. Department of Energy under Contract No. DE-FG02-91ER40626. H.P.V.'s research was supported in part by Grant No. F-460 of the Bulgarian National Research Fund. H.P.V. is thankful to the U.S. NSF for partial support of his visit to the U.S. where this work was conceived, and to the Bartol Research Institute for its hospitality.

-
- [1] D. J. Bird *et al.*, *Astrophys. J.* **441**, 144 (1995).
 - [2] N. Hayashida *et al.*, *Phys. Rev. Lett.* **73**, 3491 (1994).
 - [3] A. M. Hillas, *Annu. Rev. Astron. Astrophys.* **22**, 425 (1984).
 - [4] J. P. Rachen and P. L. Biermann, *Astron. Astrophys.* **272**, 161 (1993); J. P. Rachen, T. Stanev, and P. L. Biermann, *ibid.* **273**, 377 (1993).
 - [5] S. S. Al-Dargazelli *et al.* (unpublished); J. Szabelski, J. Wdowczyk, and A. W. Wolfendale, *J. Phys. G* **12**, 1443 (1986).
 - [6] P. Bhattacharjee, C. T. Hill, and D. N. Schramm, *Phys. Rev. Lett.* **69**, 567 (1992); G. Sigl, D. N. Schramm, and P. Bhattacharjee, *Astropart. Phys.* **2**, 401 (1994).
 - [7] E. Waxman, *Phys. Rev. Lett.* **75**, 386 (1995).
 - [8] M. Vietri, *Astrophys. J.* **453**, 883 (1995).
 - [9] M. Milgrom and V. Usov, *Astrophys. J.* **449**, L37 (1995).
 - [10] D. J. Bird *et al.*, *Phys. Rev. Lett.* **71**, 3401 (1993).
 - [11] N. Hayashida *et al.*, *J. Phys. G* **21**, 1101 (1995).
 - [12] X. Chi, J. Wdowczyk, and A. W. Wolfendale, *J. Phys. G* **18**, 1259 (1992), and references therein.
 - [13] T. Stanev *et al.*, *Phys. Rev. Lett.* **75**, 3056 (1995).
 - [14] AGASA Collaboration, N. Hayashida *et al.*, *Phys. Rev. Lett.* **77**, 1000 (1996).
 - [15] L. J. Kewley, R. W. Clay, and B. R. Dawson, *Astropart. Phys.* **5**, 69 (1996).
 - [16] F. Halzen *et al.*, *Astropart. Phys.* **3**, 151 (1995).
 - [17] See *Cosmic Rays Above 10¹⁹ eV*, Proceedings of the Workshop, Paris, France, 1992, edited by M. Boratav *et al.* [*Nucl. Phys. B (Proc. Suppl.)* **28** (1992)]; The Auger Collaboration, "The Pierre Auger Project," Design report, 1995 (unpublished).
 - [18] T. K. Gaisser *et al.*, *Phys. Rev. D* **43**, 314 (1991).
 - [19] T. J. L. McComb, R. J. Protheroe, and K. E. Turver, *J. Phys. G* **5**, 1613 (1979).
 - [20] F. A. Aharonian, B. L. Kanewski, and V. V. Vardanian, *Astrophys. Space Sci.* **167**, 111 (1990).
 - [21] T. Erber, *Rev. Mod. Phys.* **38**, 626 (1966).
 - [22] R. A. Langel, *International Geomagnetic Reference Field, 1991 Revision* (IAGA News, Langstone Press, Aberdeen, 1991), No. 30.
 - [23] B. McBreen and C. J. Lambert, in *Proceedings of the 17th International Cosmic Ray Conference*, Paris, France, 1981 (CEN, Saclay, 1981), Vol. 6, p. 70.
 - [24] H. P. Vankov and P. V. Stavrev, *Phys. Lett. B* **266**, 178 (1991).
 - [25] See T. Stanev *et al.*, *Phys. Rev. D* **25**, 1291 (1982), for the influence of the LPM effect on the shower development.